Paper-based biosensor relying on flower-like reduced graphene guided enzymatically deposition of polyaniline for Pb^{2+} detection

Shenguang Ge, Kaiqing Wu, Yan Zhang, Mei Yan, Jinghua Yu

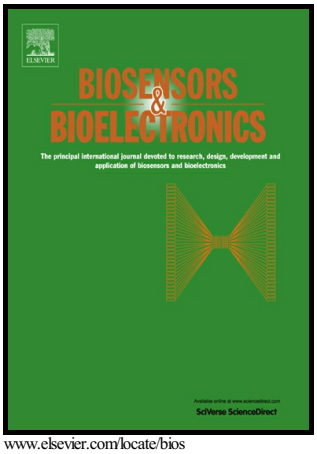

www.elsevier.com/locate/bios

PII: S0956-5663(16)30083-5
DOI: http://dx.doi.org/10.1016/j.bios.2016.01.072
Reference: BIOS8412

To appear in: *Biosensors and Bioelectronic*

Received date: 7 December 2015
Revised date: 15 January 2016
Accepted date: 28 January 2016

Cite this article as: Shenguang Ge, Kaiqing Wu, Yan Zhang, Mei Yan and Jinghua Yu, Paper-based biosensor relying on flower-like reduced graphene guided enzymatically deposition of polyaniline for Pb^{2+} detection, *Biosensor and Bioelectronic,* http://dx.doi.org/10.1016/j.bios.2016.01.072

Paper-based biosensor relying on flower-like reduced graphene guided enzymatically deposition of polyaniline for Pb^{2+} detection

Shenguang Ge[a,b], Kaiqing Wu[a], Yan Zhang[a], , Mei Yan[a], Jinghua Yu[a]*

[a] School of Chemistry and Chemical Engineering, University of Jinan, Jinan 250022 (P. R. China)

[b] Shandong Provincial Key Laboratory of Preparation and Measurement of Building Materials, University of Jinan, Jinan 250022 (P.R. China)

*Corresponding author: Jinghua Yu
E-mail: ujn.yujh@gmail.com
Telephone: +86-531-82767161

Abstract: A multi-amplified paper-based electrochemical strategy using Pb^{2+} dependent DNAzyme as the recognition unit for Pb^{2+} detection was developed. In this work, flower-like reduced graphene (FrGO) was prepared utilizing flower-like ZnO as template, which was first one step grown on the gold nanoparticles modified paper working electrode (Au-PWE). After being treated with acid and then modified with Au, a novel sensor platform named Au/FrGO/Au-PWE with large specific surface area and good electrical conductivity was fabricated. The Mn_2O_3 nanoparticle-assembled hierarchical hollow spheres (H-Mn_2O_3) was served as nanocarrier to immobilize GOx, HRP and signal strand (S3), resulting to the formation of S3/H-Mn_2O_3/HRP/GOx bioconjugations. In the presence of Pb^{2+}, the DNAzyme (S1) was activated and the substrate strand (S2) was cleaved. After the incubation with S3/H-Mn_2O_3/HRP/GOx in 0.1 M HAc-NaAc solution (pH 4.3) containing 30 mM aniline and 15 mM glucose, a readily measurable ‘‘turn-on’’ electrochemical signal could be measured. On the basis of the signal amplification strategy of Au/FrGO/Au-PWE sensing platform and S3/H-Mn_2O_3/HRP/GOx bioconjugations, the developed biosensor exhibited a good linear response toward over a wide range of concentration from 0.005 to 2000 nM.

Keywords: paper; Pb^{2+}; DNAzyme; flower-like reduced graphene.

1. Introduction

Prevention of water resources is of significance for environmental protection and human health. Inorganic contaminants such as heavy metal ions have a large impact on the ecosystem and present potential risks to human health (Vodyanitskii, 2013). Lead ion (Pb^{2+}) is one of the most toxic heavy metals contaminant to human health and the environment. Long-term exposure or excessive intake of Pb^{2+} can damage the nervous system, brain function, and other organs such as heart, kidney, and lungs (Sudhakar et al., 2012; Chen et al., 2005). Therefore, rapid and sensitive detection of Pb^{2+} is of significance for environmental protection as well as disease prevention and treatment. In recent years, several sensors have been developed for Pb^{2+} detection by fluorescence (Li et al., 2010), photoelectrochemical (Zhang et al., 2014),

electrochemiluminescence (Li et al., 2015), colorimetric (Zhu et al., 2011), and electrochemical method (Shen et al., 2008). Especially, the electrochemical methods have drawn more and more interest because of their simple instrumentation, low cost, good portability, fast response time, and the ability to provide in situ and real-time information.

Signal amplification is regarded as a vital point for sake of obtaining high sensitive biosensors. So far, various nanomaterials have been developed as nano-carriers to achieve the amplified electrochemical signal due to their extremely excellent biocompatibility, small size, special structure and large surface-to-bulk ratio (Xu et al., 2012; Lai et al., 2014; Du et al., 2010; Wang et al., 2013). Among them, metal oxide nanomaterials have drawn remarkable research interest in the past few years because of their particular chemical and physical properties. For example, Sun and co-workers have used Fe_3O_4/MnO_2 nanocomposites as promising nanocarrier of signal-amplifying nanoprobes for sensitive electrochemical biosensors (Sun et al., 2016). As a kind of metal oxide nanomaterials, manganic oxide (Mn_2O_3) was also used as anode material in lithium ion battery (Su et al., 2015), but few reports using Mn_2O_3 as nano-carrier for signal amplification in sensors. Herein, Mn_2O_3 nanoparticle-assembled hierarchical hollow spheres (H-Mn_2O_3) with large surface area were synthesized using a template as model and applied as nano-carrier in the proposed electrochemical biosensor.

For working electrode, nanoparticles have contributed a lot in increasing the sensing surface area for further developing excellent electrochemical properties (Kumar et al., 2010; Ronkainen et al., 2010; Xu et al., 2011). Unfortunately, nanomaterials with two-dimensional structure usually used to modify the working electrode, which leaded to an inherently limited surface expansion. Therefore, synthesis of nanomaterials with three-dimensional (3D) structure was significative in further increasing the surface area of electrode. Reduced graphene (rGO), as a one-atom thick sp^2-bonded carbon sheet, has been emerged as an interesting material in recent research, such as chemical and biological sensors (Sanchez et al., 2012), fuel cell (Liu et al., 2014), capacitors (Chen et al., 2013), etc., contributing to its prominent

electrical, physiochemical, and structural properties (Hu et al., 2013; Du et al., 2014). Nowadays, scientists have focused on the usage of 3D rGO in the assembly sensors. For example, Sun et al. have developed a facile electrochemical immunoassay for sensitive detection of carcinoembryonic antigen using 3D macroporous gold nanoparticles/graphene composites as platform for capturing more primary antibodies (Sun et al., 2013). Du et al. have prepared a novel graphene flowers modified carbon fiber electrode for sensitive determination of ascorbic acid, dopamine and uric acid (Du et al., 2014). Besides that, during the last years, a tremendous of articles were published utilizing paper as a novel substrate for developing simple, point-of-care assays due to its advantages, such as renewable and biocompatibility, low cost of materials, ease of device fabrication, and the ability to modify paper with a variety of reagents (Desmet et al., 2016; Cate et al., 2015). Nonetheless, there were no reports available in the literatures which synthesized multi-layered graphene on paper electrode for detecting analytes. In this work, flower-like graphene (FrGO) with large specific surface area and good electrical conductivity were synthesized on the fibres of paper through electro-reduction process.

In this report, a high-performance biosensor for the detection of Pb^{2+} based on folding paper was constructed. For biosensor fabrication, gold nanoparticles (AuNPs), FrGO and AuNPs modified paper working electrode (Au-PWE) were used as sensing platform for Pb^{2+}-dependent DNAzyme strands attachment. HRP and GOx molecules were covalently conjugated onto the surface of H-Mn_2O_3, which were used as molecular tags. Recent researches have shown that the electroactive polyaniline (PANI) could be perfectly prepared through the HRP-catalytic oxidation of aniline in a weak acid condition (Liu et al., 1999; Gao et al., 2009; Li et al., 2013). After the sandwich immunoreaction and subsequent incubation in glucose and aniline solution, the carried enzymes catalyzed oxidation polymerization of aniline to PANI on the biosensor surface, thus enhancing the conductivity of electrode. Meanwhile, enzymatic produced PANI could be electrochemically measured for the quantitative immunoassay. Results demonstrated that the method showed excellent analytical performance for Pb^{2+}, thus indicating great potentials for applications in environment

monitoring.

2. Experimental

2.1. Materials

Manganese nitrate ($Mn(NO_3)_2$), zinc nitrate hexahydrate ($Zn(NO_3)_2 \cdot 6H_2O$), tris (2-carboxyethyl) phosphine hydro-chloride (TCEP), 1-ethyl-3-(3-(dimethylamino) propyl) carbodiimide hydrochloride (EDC), N-hydroxysuccinimide (NHS), poly (diallyldimethylammonium chloride) PDDA, potassium ferricyanide, tetrachloroauric acid ($HAuCl_4 \cdot 4H_2O$, 1%, w/w), ascorbic acid (AA) were purchased from Sigma-Aldrich Chemical Co. (St. Louis, MO, USA). 6-mercapto-1-hexanol (MCH) was purchased from Nanoport. Co. Ltd. (Shenzhen, China).Hydrogen peroxide (H_2O_2, 30%, w/v) was obtained from Chemical Reagent Co. (Tianjin, China). Graphene oxide (GO) was prepared according to a modified Hummer's method by Xianfeng Nano Company (Nanjing, China). All oligonucleotides were synthesized and purified from TaKaRa Biotechnology (Dalian, China). The DNA oligonucleotide sequences were set as (S1) DNAzyme strand, (S2) substrate strand, and (S3) signal strand and listed in the supporting information. An acetic acid-sodium acetate (HAc-NaAc) buffer solution containing 30 mM aniline and 2 mM H_2O_2 were prepared and used as the enzymatic deposition solution. Trisodium citrate dehydrate were obtained from Sigma-Aldrich Chemical Co. (St. Louis, MO, USA).

All other reagents were of analytical grade and used without further purification and the water used through-out all experiments was purified through a Millipore system.

2.2. Instruments

Scanning electron microscope (SEM) images were obtained using a QUANTA FEG 250 thermal field emission scanning electron microscopy (FEI Co., USA) and utilized to characterize the modified paper and nanoparticles. Electrochemical measurements were performed on a CHI 660D electrochemistry workstation (Shanghai CH Instruments Co., China). To investigate the stepwise-modified paper

electrode, we measured the electrochemical impedance spectroscopy (EIS) of the modified paper electrode on an IM6x electrochemical station (Zahner, Germany). Energy dispersive spectrometer (EDX) was obtained using an Oxford X-MAX50 EDX (Oxford, Britain).

2.3. Preparation of FrGO/Au-PWE

AuNPs own series of merit, such as high surface area, excellent biocompatibility and extraordinary electroconductibility. At the beginning, AuNPs layer was grown on the surfaces of cellulose fibers in the hydrophilic zone of the paper to fabricate Au-PWE (details could be found in the supporting information). To fabricate the FrGO on the paper, flower-like ZnO (FZnO) template was fabricated firstly. Briefly, 1.5 g of $Zn(NO_3)_2 \cdot 6H_2O$ and 3.5 g of trisodium citrate dehydrate were dissolved in 100 mL of ultra-pure water under stirring. Then the Au-PWE was soaked in the above mixed solution. After stirred for 30 min, 20 mL of NaOH solution (1.25 M) was added into the mixed solution and sequentally stirred for 3 h at room temperature. Subsequently, the resulting FZnO/Au-PWE was thoroughly washed with ethanol and water and repeated five times. In the end, the product was obtained with the procedure of drying at 80 °C for one night. Before the electro-reduction process, GO was suspended and adjusted to 1 $mg \cdot mL^{-1}$. Then the FZnO/Au-PWE was immersed in GO solution and electrochemically reduced at a constant potential of 0.9 V in 0.1 M Na_2SO_4. After the electro-reduction process, the GO-FZnO/Au-PWE was treated with hydrochloric acid (0.5 M) to remove the ZnO template. The resulting FrGO/Au-PWE electrodes were washed with ultrapure water four times and stored at 4 °C before use.

2.4. Preparation of H-Mn_2O_3 and S3/Mn_2O_3/HRP/GOx

The synthetic procedures of H-Mn_2O_3 were based on the reported methods with appropriate modifications (Cheng et al., 2015). Briefly, 1.0 g of glucose was added into 40.0 mL $Mn(NO_3)_2$ (0.6 M) solution under magnetic stirring for ten minutes, produced a homogeneous solution. Subsequently, the resulting solution was transferred into a Teflon-lined stainless-steel autoclave, which was then sealed and

heated at 180 ° C for 18 h. After cooling to room temperature, the black product was centrifuged and washed with ethanol; the process was repeated three times. Afterward, the precursor was obtained via drying the black product at 80° C overnight, and the precursor was calcined at 600 °C for 4 h in an oven to obtain the final H-Mn_2O_3.

The typical preparation process for S3/H-Mn_2O_3/HRP/GOx was as follows. In total, 10 mg of as-prepared H-Mn_2O_3 was treated with a mixture of H_2SO_4/HNO_3 (volume ratio 3:1), followed by sonicating for 2 h. After that, suspension was centrifuged and washed with ultrapure water four times until the pH was neutral. The resulting carboxylic-functionalized H-Mn_2O_3 was dried under vacuum overnight and then dispersed in 5 mL water followed by sonicating for 10 min. Afterwards, 1 mL of 400 mM EDC and 100 mM NHS was injected into 1mL of the dispersion, and swirled at room temperature for 1h to give a homogenous suspension. Subsequently, GOx(2.0 $mg{\cdot}mL^{-1}$) and HRP (3.0 $mg{\cdot}mL^{-1}$) were added into the suspension followed by gently shaking at 4 °C for 5 h to make protein molecules assemble to H-Mn_2O_3. Finally, the resulting H-Mn_2O_3/HRP/GOx bioconjugations were obtained after being centrifuged and washed.

To achieve the conjugation between S3 and H-Mn_2O_3/HRP/GOx, the signal strand (S3) was firstly activated with an acetate buffer (pH 5.2) and 1.5 μL of 10 mM TCEP for 1 h at room temperature. Then 300 μL of as-prepared H-Mn_2O_3/HRP/GOx conjugates were incubated with S3 for 6 h under slight shaking. 100 μL of 1% BSA solution was blocked for 1 h to block the remaining active sites at room temperature. The unbound proteins were removed by successive centrifugation and washing with ultrapure water several times. The bioconjugation were dispersed in Tris-HCl (10 mM, pH 7.4) buffer and stored at 4 °C.

2.5. Fabrication of electrochemical biosensor

The fabrication and the assay procedure for the Pb^{2+} biosensor were represented in Scheme 1. Firstly, 10 μL of 0.5% PDDA aqueous solution containing 0.5 M NaCl was dropped on the as-prepared FrGO/Au-PWE. After incubating for 10 min, 5 μL AuNPs (details could be found in the supporting information) were dropped on the surface of

the working electrode. Subsequently, the modified working electrode was incubated with DNAzyme strands (S1, 10.0 μL, 1.0 mM) for 6 h at 37 °C. After washing three times with a stream of Tris-HCl buffer (10mM, pH 7.4), 0.2 mg MCH was added and incubated for 30 min to resist the nonspecific adsorption of the DNAzyme-modified electrode and then rinsed with Tris-HCl buffer (10mM, pH 7.4). Subsequently, substrate strand (S2, 10.0 μL, 1.0 mM) was dropped on the electrode and incubated in a 65 °C water bath for 10 min. After the hybridization reaction, the electrode was exposed in air and gradually cooled down to room temperature. Various concentrations of Pb^{2+} was introduced in the modified electrode and allowed to react for 1 h at room temperature. In the presence of Pb^{2+}, the DNAzyme was activated and cleaved the substrate strand, producing free DNAzyme strand and two fragments, respectively. After being thoroughly rinsed with the washing buffer, the Au/FrGO/Au-PWE/S1/BSA/Pb^{2+} electrode was completed and ready for further use. To realize the signal amplification, the synthesized S3/H-Mn_2O_3/HRP/GOx signal strand (0.5 μM) was incubated with the electrode at room temperature for 30 min. After hybridization, the electrode was extensively rinsed with Tris-HCl buffer (10mM, pH 7.4) and dried under a stream of nitrogen prior to electrochemical characterization.

(Scheme 1)

2.6. Electrochemical detection

The biosensor was immersed in 0.1 M HAc–NaAc solution (pH 4.3) containing 30 mM aniline and 15 mM glucose to form PANI at room temperature. Differential pulse voltammetry (DPV) measurements were performed in Tris-HCl buffer (10mM, pH 7.4) and potential swept from -0.5-0.4V with scanning rate of 100 mV s^{-1}.

3. Results and discussion

3.1. Characterization of FrGO/Au-PWE, H-Mn_2O_3

The Au-PWE was developed through the growth of AuNPs layer on the paper sample zone, which could enhance the conductivity of paper sample zone. As shown in Fig. 1A, interconnected and continuous AuNPs layer with high area was got on the

rough and porous cellulose fibers surfaces (Fig. 1B). Fig. 1B showed that a large number of FZnO were distributed on the surface of Au-PWE with an average size of 2 μm. The FZnO displayed a large spatial structure, which was similarly mosaicked by platy ZnO. After the electroreduction of GO, a layer of FrGO was deposited on the surface of FZnO/Au-PWE (Fig. 1C). As displayed by the SEM measurements, after the removal of ZnO template by hydrochloric acid treatment, graphene covered wholly and uniformly on the surface of electrode with lots of ripples (Fig. 1D). It could be believed that the graphene flowers increased the surface area of electrode.

The morphology of the as-synthesized product was investigated by SEM. Fig. 2A showed that the image displayed a type of spherical morphology and homogeneous dispersion of the precursor with a diameter of ~1 μm. The precursor could be regarded as the carbon spheres template loaded with Mn(II) ions. After the calcination of the precursor, H-$Mn_2O_3$was obtained as a result. SEM image confirmed that H-Mn_2O_3 (~500 nm) were spherical morphology with a rough surface as depicted in Figure 2B, indicating that the H-Mn_2O_3 was formed by aggregated small primary particles. The corresponding EDS of the two particles were shown in Figure 2C and Figure 2D, respectively. Results indicated the successful synthesis of precursor and H-Mn_2O_3. We confirmed that the final product was H-Mn_2O_3 rather than MnO_2 because the formation of high-valence manganese oxide would be hindered by carbon spheres, which possessed reductive properties (Cheng et al., 2015).

(Fig. 1)

(Fig. 2)

3.2. Characterizations of the stepwise modified electrode

To characterize the immunoarray process, EIS as a powerful tool for probing the interface features and the electron-transfer resistance at the electrode surface was recorded at different stages (Li et al., 2009; Qiu et al., 2016). The EIS spectra is presented as Nyquist plots, which commonly include a semicircle region lying on the axis followed by a straight line. Moreover, the semicircle diameter equals the electron-transfer resistance, R_{et}. Fig. S1A showed a Nyquist plot of impedance for the

stepwise modification process with the Au-PWE. It was observed that bare PWE exhibited a relatively small semicircle at high frequencies and a linear part at low frequencies (curve a). After the growth of AuNPs layer, the Au-PWE showed a lower resistance (curve b). While FrGO was attached on the Au-PWE (curve c), no significant change was found in resistance when compared with curve b. The diameter of the semicircle part continued decreased after the AuNPs were modified onto the electrode surface (curve d). After immobilization of S1, the value of R_{et} increased (curve e), which was due to the negatively charged S1 on the electrode surface electrostatically repelled the negatively charged redox probe $[Fe(CN)_6]^{3-/4-}$ and inhibited interfacial charge transfer as an insulating protein layer (Hou et al., 2013).

The cyclic voltammetry (CV) was chosen to investigate the change of electrode behavior after each assembly step. Fig. S1B showed the CVs of different modified eletrodes in Tris-HCl (10 mM, pH 7.4) containing 0.1 M KCl and 5 mM $[Fe(CN)_6]^{3-/4-}$ from -0.2 to 0.8 V (vs. SCE) at a scan rate of 100 mVs^{-1}. It was found that the bare PWE exhibited one set of well defining redox peaks (curve a). After the modification of an AuNPs layer in PWE, there was an obvious increase of the peak current (curve b), indicated that the porous Au-PWE had a much larger effective surface area. The high enhanced peak current was attributed to the high conductivity of Au, which made electron transfer easier. After the polymerization of FrGO on the surfaces of Au-PWE, the peak current of the CV curves (curve c) increased compared with the Au-PWE, which indicated that the FrGO could offer high surface area and good conductivity in the electrode. In addition，the introduction of AuNPs also increased the peak current (curve d). After S1 and BSA were successively adsorbed onto the electrode surface (curves e–f, respectively), an obvious decrease in the signal was observed, which was owing to the conjugated protein layers that obstructed the electron transport.

The electrochemical response was induced by the deposition of PANI. To verify the conception, the CVs were used to characterize different eletrodes in Tris-HCl (10 mM, pH 7.4) buffer at a scan rate of 100 mV s^{-1}. No redox peaks were observed in Au/FrGO/Au-PWE/S1 (Fig. 3A, curve a), Au/FrGO/Au-PWE/S1/BSA (Fig. 3A, curve b) and Au/FrGO/Au-PWE/S1/BSA/Pb^{2+}/S3/H-Mn_2O_3/HRP/GOx (Fig. 3A, curve c),

indicating that there was no substance with electrochemical activity in the electrodes and solution. In contrast, Au/FrGO/Au-PWE/S1/BSA/Pb^{2+}/S3/H-Mn_2O_3/HRP/GOx electrode was immersed into 0.1 M HAc–NaAc solution (pH 4.3) containing 30 mM aniline and 15 mM glucose. After keeping for 20 min reaction, the electrode was rinsed with 0.1 M HAc–NaAc solution (pH 4.3) and then transferred into a Tris-HCl (10 mM, pH 7.4) buffer to perform electrochemical measurement. As could be seen in Fig. 3A, Au/FrGO/Au-PWE/S1/BSA/Pb^{2+}/S3/H-Mn_2O_3/HRP/GOx electrode revealed a pair of well-defined redox peaks (curve d) in the working potential range. The results indicated that the signal was generated relying on the efficient redox activity of PANI. Meanwhile, the result clearly demonstrated that PANI had been successfully generated through the catalytic reaction of the S3/H-Mn_2O_3/HRP/GOx bioconjugation. The concentration of Pb^{2+} was 1 nM.

To clarify the FrGO can offer a larger electro-active surface area, CVs of variously modified electrode was measured to probe the feature of different modified electrode surface. A pair of well-defined redox peaks appeared when the Au-PWE was immersed in PBS (pH 7.4) containing 0.1 M KCl and 5 mM $[Fe(CN)_6]^{3-/4-}$ from -0.2 to 0.8 V (vs. SCE) at a scan rate of 100 mVs^{-1} (Fig 3B, curve a). An obviously enhanced current signal was observed when using the usual graphene modified Au-PWE (G/Au-PWE, curve b), which was prepared using the same procedures as described in section 2.2 without adding FZnO template. Compared with the Au-PWE and G/Au-PWE, the FrGO/PWE exhibited the most significant increased current (curve c). The results demonstrated that FrGO modified electrode had larger electroactive surface area and could promote the electron transfer better compared with usual graphene modified electrode, which was ascribed to the special wrinkle nanostructures.

(Fig. 3)

3.3. Electrochemical determination of Pb^{2+}

Because the amount of HRP/GOx is depended on the concentration of Pb^{2+}, the amount of H_2O_2 is dependent on the amount of HRP/GOx, and the generated PANI

consumes the H_2O_2 generated in the system, so that the electrochemical response signal of PANI increased with the increasing Pb^{2+} concentration. DPV, a sensitive analytical technique, was used for studying the electrochemical changes here. Under the optimal conditions (detail can be found in supporting information), the DPV responses of the biosensor increased with increasing concentrations of pb^{2+} (Figure 4A). The calibration plot showed a good linear relationship between the peak currents and the logarithm values of the analyte concentrations in the range from 0.005 to 2000 nM. The linear regression equation was expressed as $I = -6.7182-2.8233lg[Pb^{2+}]$ ($[Pb^{2+}]$, nM) with a correlation coefficient of 0.996 (Figure 4B). In consequence, a low detection limit of 0.002 nM was evaluated using a signal three-fold of the background noise.

To further clarify the sensitivity and acceptability of the as-proposed Pb^{2+} biosensor based on the novel FrGO/Au-PWE, the comparison between the as-prepared biosensor and other Pb^{2+} biosensors was listed in (Table S1). Results showed that the developed biosensor possessed higher sensitivity and could be used for the practical detection of Pb^{2+}.

(Fig. 4)

3.4. Stability and specificity of the biosensor

A key factor of the sensor in their application and development is the stability. The as-prepared Pb^{2+} biosensor was stored in the refrigerator (4 °C) for a week, and almost no signal intensity was changed significantly. Furthermore, the storage time was prolonged to four weeks. Over 90.0% of original responses were retained after such long time, indicating that the Pb^{2+} biosensor had acceptable storage stability.

While the sensor was applied to the Pb^{2+} analysis, the specificity of the biosensor must be validated to ensure that the sensor was acceptable. Several other metal ions, such as Ca^{2+}, Zn^{2+}, Mg^{2+}, Cu^{2+}, Hg^{2+}, Ag^{+}, K^{+}, Na^{+}, Cr^{3+}, Al^{3+} and Fe^{3+}, were tested as a control. The current responses of the as proposed biosensor, which was incubated with 10 nM Pb^{2+} and other competing metal ions with same concentration in real samples, was shown in Figure S3. The peak current value of competing metal ions

were close to the blank solution and far from the value of Pb^{2+}, which indicated that the developed biosensor exhibited a high selectivity to Pb^{2+}. Such excellent selectivity is attributed to the specific DNAzyme for the pairing of Pb^{2+}. Therefore, the as-prepared Pb^{2+} biosensor was suitable to apply for the detection Pb^{2+}.

3.5. Application of the biosensor in lake water

Pb^{2+} in the freshwater system is the most common lead pollution in the environment. To carry out the practical application of the proposed biosensor, lake water was prepared by simply filtered firstly. Then, 10 μL of lake water samples spiked with different concentrations of Pb^{2+} was added to the biosensor. As shown in Table 1, the recovery values were 94.0%, 97.1% and 103.2%, indicating that the acceptable accuracy of the proposed biosensor for the practical detection of Pb^{2+} in real samples.

(Table 1)

4. Conclusion

In the system, we have developed a sensitive Pb^{2+} biosensor using Au/FrGO/Au-PWE as amplified signal sensing platform and S3/H-Mn_2O_3/HRP/GOx as amplified signal tag. The FrGO with large specific surface area and good electrical conductivity was synthesized on the fibres of paper through an electro-reduction process. S3/H-Mn_2O_3/HRP/GOx was used for the catalyzed deposition of PANI, which possessed efficient redox activity and could be electrochemically measured. Compared with the detection performance of conventional Pb^{2+} sensing strategies, the proposed biosensor showed high sensitivity, good stability, acceptable reproducibility in Pb^{2+} detection attributing to the signal amplification of S3/H-Mn_2O_3/HRP/GOx and the electron transfer acceleration of Au/FrGO/Au-PWE. This method could be expanded readily for detecting other metal ions in public and environmental safety.

Acknowledgments

This work was financially supported by Special Fund for Shandong Independent

Innovation and Achievements Transformation (No. 2014ZZCX02703), National Natural Science Foundation of China (21475052, 21277058).

Appendix A. Supplementary information

References

Cate, D. M., Adkins, J. A., Mettakoonpitak, J., Henry, C. S., 2015. Anal. Chem. 87, 19-41.

Chen, J., Li, C., Shi, G. Q., 2013. J. Phys. Chem. Lett. 4, 1244-1253.

Chen, P., Greenberg, B., Taghavi, S., Romano, C., van der Lelie, D., He, C., 2005. Angew. Chem. Int. Edit. 44, 2715-2719.

Cheng, C. M., Huang, Y., Wang, N., Jiang, T., Hu, S., Zheng, B. Z., Yuan, H. Y., Xiao, D., 2015. ACS Appl. Mater. Interfaces 7, 9526-9533.

Desmet, C., Marquette, C. A., Blum, L. J., Doumèche, B., 2016. Biosens. Bioelectron. 76, 145-163.

Du, D., Zou, Z. X., Shin, Y. S., Wang, J., Wu, H., Engelhard, M. H., Liu, J., Aksay, I. N., Lin, Y. H., 2010. Anal. Chem. 82, 2989-2995.

Du, J., Yue, R. R., Ren, F. F., Yao, Z. Q., Jiang, F. X., Yang, P., Du, Y. K., 2014. Biosens. Bioelectron. 53, 220-224.

Gao, Z.Q., Rafea, S., Lim, L.H., 2007. Adv. Mater. 19, 602-606.

Hu, Y., Xue, Z., He, H., Ai, R., Liu, X., Lu, X., 2013. Biosens. Bioelectron. 47, 45-49.

Hou, L., Cui, Y. L., Xu, M. D., Gao, Z. Q., Huang, J. X., Tang, D. P., 2013. Biosens. Bioelectron. 47, 149-156.

Kumar, S.A., Wang, S.F., Yang, T.C.K., Yeh, C.T., 2010. Biosens. Bioelectron. 25, 2592-2597.

Lai, G. S., Zhang, H. L., Tamanna, T., Yu, A. M., 2014. Anal. Chem. 86, 1789-1793.

Li, F., Yang, L. M., Chen, M. Q., Qian, Y., Tang, B., 2013. Biosens. Bioelectron. 41, 903-906.

Li, M., Kong, Q. K., Bian, Z. Q., Ma, C., Ge, S. G., Zhang, Y., Yu, J. H., Yan, M.,

2015. Biosens. Bioelectron. 65, 176-182.

Li, T., Dong, S.J., Wang, E.K., 2010. J. Am. Chem. Soc. 132, 13156-13157.

Li, X.H., Dai, L., Liu, Y., Chen, X.J., Yan, W., Jiang, L.P., Zhu, J.J., 2009. Adv. Funct. Mater. 19, 3120-3128.

Liu, M. M., Zhang, R. Z., Chen, W., 2014. Chem. Rev. 114, 5117-5160.

Liu, W., Kumar, J., Tripathy, S., Senecal, K. J., Samuelson, L., 1999. J.Am. Chem. Soc. 121, 71-78.

Qiu, Z. L., Tang, D. Y., Shu, J., Chen, G. N., Tang, D. P., 2016. Biosens. Bioelectron. 75, 108-115.

Ronkainen, N.J., Halsall, H.B., Heineman, W.R., 2010. Chem. Soc. Rev. 39, 1747-1763.

Sanchez, V. C., Jachak, A., Hurt, R. H., Kane, A. B., 2012. Chem. Res. Toxicol. 25, 15-34.

Sun, D. P., Lu, J., Zhong, Y. W., Yu, Y. Y., Wang, Y., Zhang, B. B., Chen, Z. G.,2016. Biosens. Bioelectron. 75, 301-307.

Su, H., Xu, Y. F., Feng, S. C., Wu, Z. G., Sun, X. P., Shen, C. H., Wang, J. Q., Li, J. T., Huang, L., Sun, S. G., 2015. ACS Appl. Mater. Interfaces 7, 8488-8494.

Sudhakar, G. K., Verma, R., Kurba, V. B., Kumar, L., 2012. Int. Res. J. Pharm. 3, 128-130.

Shen, L., Chen, Z., Li, Y.H., He, S.L., Xie, S.B., Xu, X.D., Liang, Z.W., Meng, X., Li, Q., Zhu, Z.W., Li, M.X., Le, X.C., Shao, Y.H., 20 08. Anal. Chem. 80, 6323-6328.

Sun, G. Q., Lu, J. J., Ge, S. G., Song, X. R., Yu, J. H., Yan, M., Huang, J. D., 2013. Anal. Chim. Acta 775, 85-92.

Vodyanitskii, Y. N., 2013. Eurasian Soil Sci. 46, 793-801.

Wang, L. S., Lei, J. P., Ma, R. N., Ju, H. X., 2013. Anal. Chem. 85, 6505-6510.

Xu, Q. N., Yan, F., Lei, J. P., Leng, C., Ju, H. X., 2012. Chem. Eur. J. 18, 4994-4998.

Xu, S. J., Liu, Y., Wang, T. H., Li, J. H., 2011. Anal. Chem. 83, 3817-3823.

Zhang, B. T., Lu, L. L., Hu, Q. C., Huang, F., Lin, Z., 2014. Biosens. Bioelectron. 56, 243-249.

Zhu, X., Gao, X. Y., Liu, Q. D., Lin, Z. Y., Qiu, B., Chen, G. N., 2011. Chem.

Commun. 47, 7437-7439.

Figure captions

Scheme 1. Schematic illustration of the stepwise Pb^{2+} biosensor fabrication process.

Fig. 1. SEM images of (A) Au-PWE (inset: pure cellulose paper), (B) FZnO/Au-PWE (inset: magnification of image B), (C) rGO/ FZnO/Au-PWE and (D) FrGO/Au-PWE.

Fig. 2. SEM images of (A) precursor and (B) H-Mn_2O_3, EDS of (C) precursor and (D) H-Mn_2O_3.

Fig. 3. (A) CVs of different electrodes in Tris-HCl (10 mM, pH 7.4) buffer at a scan rate of 100 mV s^{-1}: (a) Au/FrGO/Au-PWE/S1, Au/FrGO/Au-PWE/S1 (b) blocked with BSA, incubated with (c) S3/H-Mn_2O_3/HRP/GOx in presence of Pb^{2+}(1 nM), (d) the electrode 'c' after reaction in 0.1 M HAc–NaAc solution (pH 4.3) containing 30 mM aniline and 15 mM glucose. (B) CVs of different electrodes in Tris-HCl (10 mM, pH 7.4) containing 0.1 M KCl and 5 mM $[Fe(CN)_6]^{3-/4-}$ from at a scan rate of 100 mV s^{-1}: (a) Au-PWE, (b) G/Au-PWE and (c) FrGO/Au-PWE.

Fig. 4. (A) DPV responses of the biosensor toward different concentrations of Pb^{2+} from 0.005nM to 2000 nM in Tris-HCl (10 mM, pH 7.4) buffer. (B) Relationship between peak currents and Pb^{2+} concentration in Tris-HCl (10 mM, pH 7.4) (inset, linear relationship between the peak currents and logarithm values of the Pb^{2+} concentrations).

Table captions

Table 1. The analysis of Pb^{2+} in lake water samples.

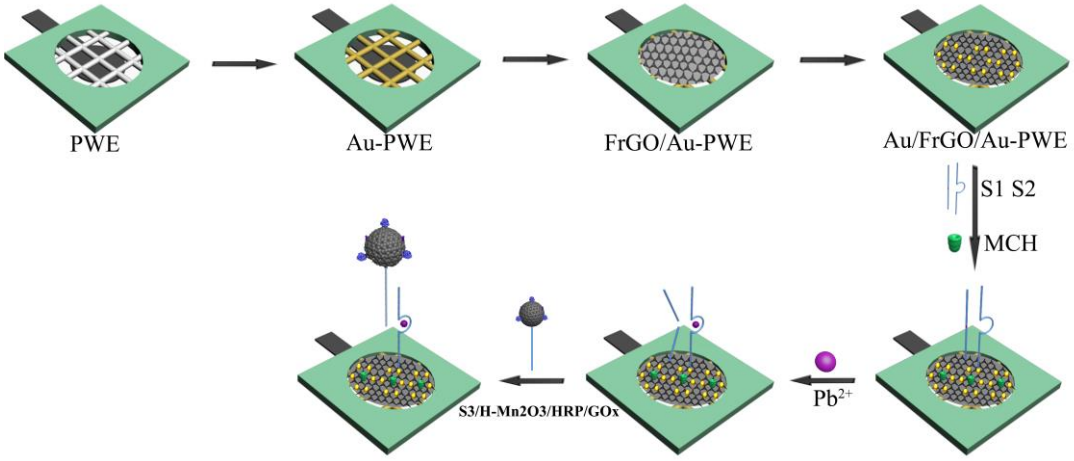

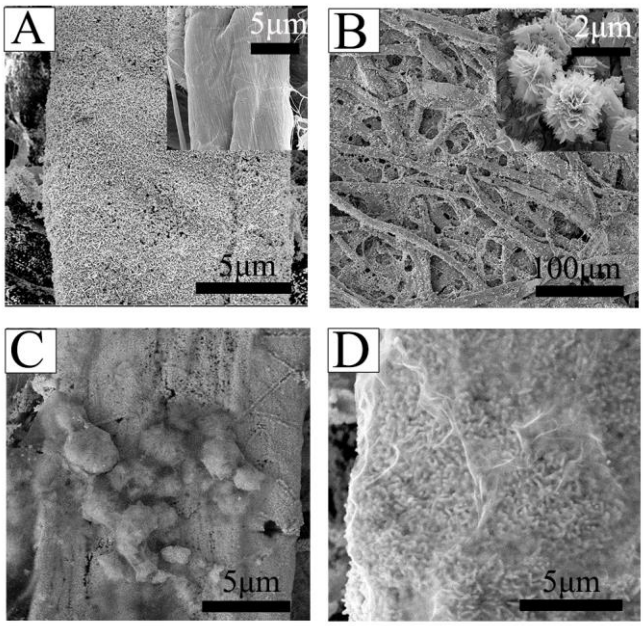

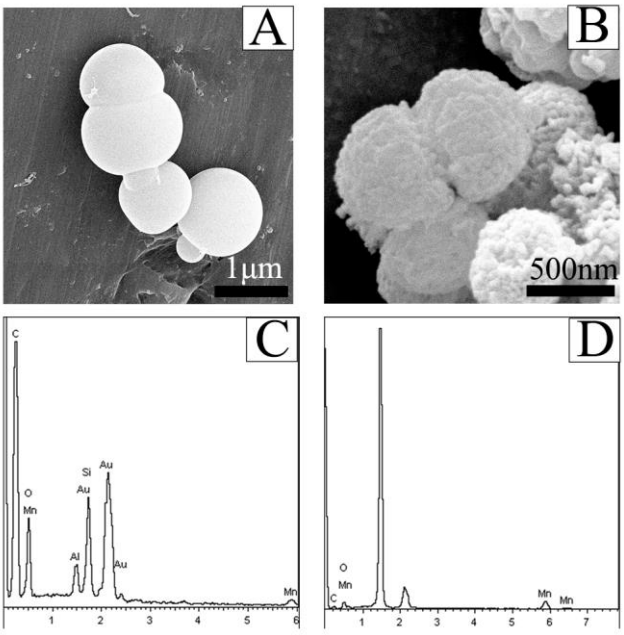

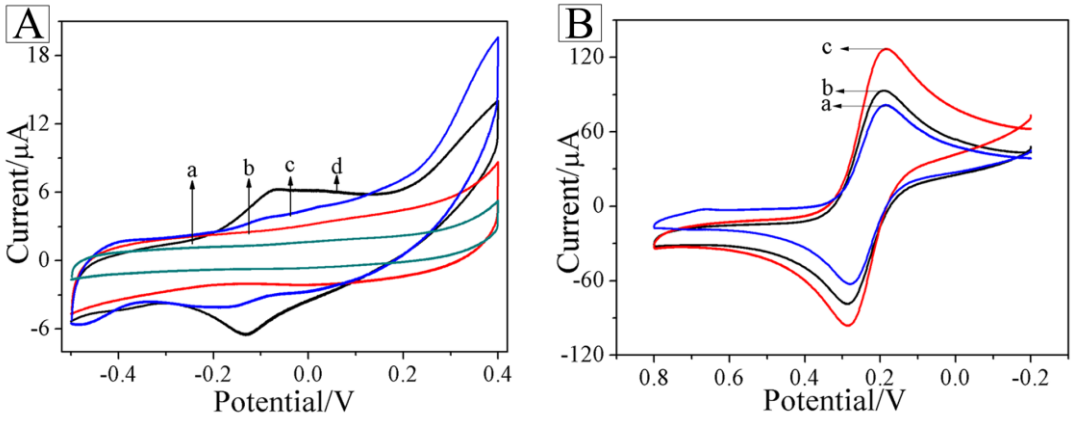

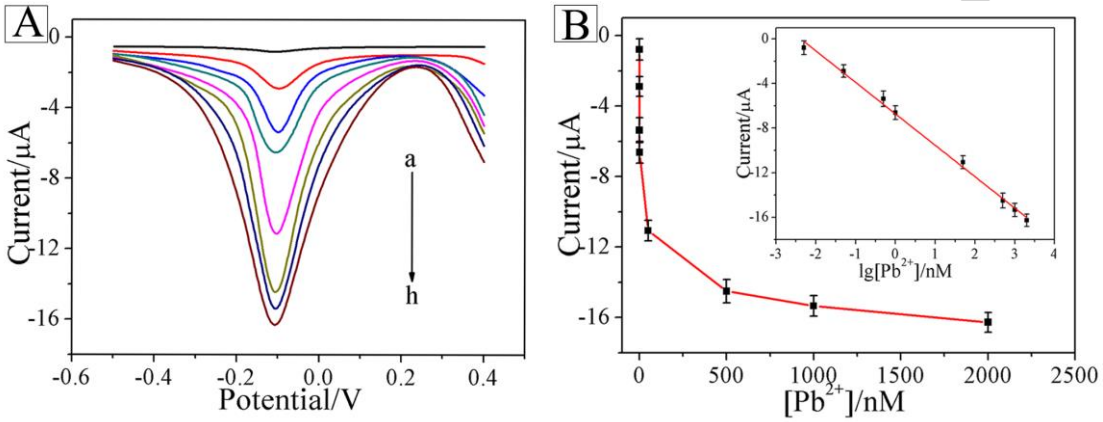

Table 1. The analysis of Pb^{2+} in lake water samples [a]

Sample	Add/nM	Found/nM	Recovery/%
lake water	0.5	0.47	94.0±4.8
	50.0	48.54	97.1±2.2
	100.0	103.20	103.2±2.5

[a] The results are expressed as mean value based on three replicates (n=3) determinations.

Highlights

1 A paper-based electrochemical strategy using Pb^{2+} dependent DNAzyme for Pb^{2+} detection was developed.

2 Flower-like reduced graphene was guided the enzymatically deposition of polyaniline.

3 The H-Mn_2O_3 was served as nanocarrier to immobilize GOx, HRP and signal strand.